

# Experience of 500 cardiovascular magnetic resonance imaging and systematic analysis of cases

 Sercin Ozkok,<sup>1</sup>  Ilker Kemal Yucel,<sup>2</sup>  Ahmet Sasmazel,<sup>3</sup>  Ahmet Celebi<sup>2</sup>

<sup>1</sup>Department of Radiology, Istanbul Medeniyet University, Goztepe Training and Research Hospital, Istanbul, Turkiye

<sup>2</sup>Department of Pediatric Cardiology, Dr. Siyami Ersek Thoracic and Cardiovascular Surgery Training and Research Hospital, Istanbul, Turkiye

<sup>3</sup>Department of Pediatric Cardiovascular Surgery, Dr. Siyami Ersek Thoracic and Cardiovascular Surgery Training and Research Hospital, Istanbul, Turkiye

## ABSTRACT

**OBJECTIVE:** Cardiovascular magnetic resonance imaging (MRI) is a widely accepted reference imaging technique in routine cardiology clinics in many centers due to its advantages in providing preferable functional, morphologic information. However, there is little information about national experience in clinical application and findings of cardiovascular MRI. The objective of this study was to demonstrate the clinical and demographic characteristics of patients admitted to our cardiac imaging department.

**METHODS:** A total of 500 cardiovascular MRI examinations performed between 2016 and 2019 were enrolled in this retrospective study. Clinical indications, demographic, and cardiovascular MRI findings of the patients were retrospectively evaluated.

**RESULTS:** Five hundred patients (M/F=301/199) were included in this retrospective, single center study. The majority of the examinations were performed for the assessment of congenital heart disease (n=254, 50.8%). The other indications were for myocardial disease (n=160, 32%), cardiac mass (n=44, 8.8%), valvular heart disease (n=20, 4%), magnetic resonance angiography (n=12, 2.4% for aorta and pulmonary artery [n=9, 1.8%] and for coronary arteries [n=3, 0.6%]), and vasculitis (n=7, 1.7%), pericardial disease (n=3, 0.6%). Minor complication was seen during the contrast agent injection in three patients (0.06%).

**CONCLUSION:** Cardiovascular MRI is a reliable and accurate imaging tool in identifying the various cardiac pathology with widely accepted use in the clinical area. Our single-center experience of 500 cases demonstrates the varieties of clinical indications in daily practice that may contribute to the national data pool.

*Keywords:* Cardiac mass; cardiomyopathy; cardiovascular magnetic resonance imaging; congenital heart disease; magnetic resonance angiography.

**Cite this article as:** Ozkok S, Yucel IK, Sasmazel A, Celebi A. Experience of 500 cardiovascular magnetic resonance imaging and systematic analysis of cases. *North Clin Istanbul* 2023;10(1):108–121.

Cardiovascular magnetic resonance imaging (MRI) has been rapidly developing over the last decades by the improvement in imaging sequence, machine design, and image quality. As a result, cardiovascular MRI is accepted as a gold-standard, non-invasive imaging technique

for measuring left and right ventricular volumes and ejection fraction. It is also approved as the best imaging technique to assess the location and severity of the myocardial scar formation and is being accepted as a gold-standard technique for the evaluation of myocardial viability [1–4].

Received: December 01, 2021

Revised: January 19, 2022

Accepted: February 23, 2022

Online: February 16, 2023

Correspondence: Sercin OZKOK, MD. Istanbul Medeniyet Universitesi, Goztepe Egitim ve Arastirma Hastanesi, Radyoloji Klinigi, Istanbul, Turkiye.

Tel: +90 216 606 52 00 e-mail: sercinbas2005@gmail.com

© Copyright 2023 by Istanbul Provincial Directorate of Health - Available online at www.northclinist.com



Although the clinical use of cardiovascular MRI may vary among centers, it is widely used in routine clinical practice. The main clinical indications of cardiovascular MRI are cardiomyopathy, myocarditis, ischemic heart disease, cardiac masses, valvular heart diseases, and vascular pathologies (aortic disease, coronary artery disease, etc.), pericardial pathology [5]. It has an essential clinical value in diagnosis and monitoring the response to the therapy of such various heart diseases. Another expanding patient group referred to cardiovascular MRI is congenital heart disease (CHD) in either pediatric and adult ages. Cardiovascular MRI has the capability to become the reference imaging technique tool for clinical follow-up or surgical decisions with the advantage of its serial application. Assessment of detailed morphologic and anatomic structure, managing post-operative complications, guidance to interventional procedures are the most common indications for referrals of cardiovascular MRI in CHD [6–8].

Cardiovascular MRI is widely used in routine cardiology practice and benefits from a multidisciplinary approach involving radiologists, radiographers, cardiologists, and cardiothoracic surgeons. Yet, national experience demonstrating clinical advantage, application, and findings of cardiovascular MRIs are sparse. The present study is designed to illustrate the demographic, clinical, and radiological characteristics of patients admitted to our cardiac imaging department with the largest patient cohort in the Turkish literature. We believe that demonstration of the findings and clinical application will enhance the use of cardiovascular MRI in daily routine.

## MATERIALS AND METHODS

Ethical approval of this retrospective study was obtained from the Istanbul Medeniyet University Clinical Research Ethics Committee (No: 2018/0483). This study was conducted in accordance with principles for human experimentation as defined in the Declaration of Helsinki. Informed consent for cardiovascular MRI examination was obtained from all patients and parents under 18 years old before the examination.

### Study Group

In this study, a total of 500 patients who underwent cardiovascular MRI imaging between 2015 November and 2018 December were retrospectively reviewed. Patient demographic data were obtained from the hospital in-

### Highlight key points

- Cardiovascular MRI is a gold-standard, non-invasive imaging technique in quantitative assessment of ventricular volume and function, blood flow, and tissue characterization.
- The majority of the examinations were performed for the assessment of CHD (50.8%). The other indications were for myocardial disease, cardiac mass, valvular heart disease, vascular, and pericardial disease.
- Cardiovascular MRI has the capability to become the reference imaging technique tool for diagnosis, follow-up or surgical decision of various cardiac pathologies with the advantage of its serial application and guiding to interventional procedures.

formation system. All the individuals had transthoracic two-dimensional echocardiography before the cardiovascular MRI examination. The echocardiography and cardiac catheter findings of the individuals were used only to determine the primary diagnosis and guide to the cardiovascular MRI.

All patients were evaluated for claustrophobia and the presence of contraindications, including MRI non-compatible implants, pacemakers, and excluded from the examination.

### Cardiac MRI Technique and Protocol

All cardiovascular MRI examinations were performed using a 1.5-Tesla scanner (Signa HDx; GE Medical Systems, Milwaukee, WI, USA) with a 32-channel phased-array abdominal coil with electrocardiographic gating. Intravenous sedation was not administered during the examination. All the patients were trained how to take a breath before the examination. The weight and height of the patients were recorded before the examination to calculate body surface area to index ventricular volume.

All examinations were performed by two technologists and 10 years experienced radiologist trained in congenital cardiac imaging. After three plane localizers through thorax revealed by steady-state free precession sequence, cine-steady state free precession sequence of two-chambers, four-chambers, and short-axis views (Protocol 1) was revealed for all patients. Each set of images was acquired with retrospective gating and 20 reconstructed cardiac phases. All the images were acquired during one or two breath-hold of 8 to 12 s duration depending on the heart rate during end-expiratory breath-hold.

A 0.2 mmol/kg of gadolinium-based contrast agent was performed if the imaging protocol was required. Contrast agent material was used for magnetic resonance angiography (MRA) for great vessels (Protocol 3), myocardial late gadolinium enhancement (Protocol 4), tissue characterization (Protocol 5), perfusion imaging (Perfusion 6), and vasculitis assessment (Protocol 8). Contrast-enhanced MRA was used to prescribe the phase-contrast imaging of the pulmonary artery, aorta. The optimal velocity encoding value of the pulmonary artery was calculated by the calculation Bernoulli equation reported gradients in the echocardiography report. Late gadolinium enhancement sequences were revealed after 10 and 15 min of injection for the assessment of myocardial disease.

Protocols 1–4 were applied for the patients with the indication of CHD. Protocols 1, 3, and 4 were applied for the patients with the indication of myocardial disease, and Protocols 1 and 7 were applied for myocardial iron assessment. Protocols 1, 5, and 6 were applied for the patients with the indication of cardiac mass. Protocols 1, 2, 3, and 4 were applied for valvular disease; protocols 1, 2, 3, 4, and 5 were applied for pericarditis; protocols 1 and 9 were applied for coronary artery assessment; and protocols 1 and 3 were applied for MRA of great vessels.

Our institutional standardized cardiovascular MRI protocol demonstrated with imaging parameters was performed (Table 1).

### Cardiac MRI Evaluation

All cardiovascular MRI examinations were retrospectively reviewed by a 10-year experienced radiologist trained in congenital cardiac imaging, with an experience of more than 1000 cardiovascular MRI examinations. All the images were reviewed using a commercially available software program (5.6i report card, GE Medical Systems, Milwaukee, WI, USA) on a workstation.

The endocardial layer of ventricles was contoured manually on short-axis cine images by including the papillary muscles and the trabeculations through all slices on end-diastolic and end-systolic phases. Body surface area (with Mosteller's formula), biventricular end-diastolic volume index, end-systolic volume index, stroke volume index, and ejection fraction were calculated automatically by the workstation.

In the flow analysis, the contour of the vascular structures was traced manually. Forward flow volume, regurgitant flow volume, and net flow volumes were calculated by a software program. Pulmonary regurgitation fraction

(regurgitant flow volume/forward flow volume  $\times$  100 in %) and blood flow distribution of the right-to-left pulmonary artery (net right pulmonary artery flow volume/[right pulmonary artery+left pulmonary artery flow volume]  $\times$  100 in %) were also calculated. The presence of end-diastolic antegrade flow was also recorded from flow diagrams. The systemic-to-pulmonary flow ratio was calculated to assess the degree of the left-to-right shunt. It was calculated as dividing the net flow volume of the pulmonary artery to ascending aorta.

MRI of each patient with CHD was analyzed for morphological information such as chamber and valve anatomy, structure and integrity of septum, alignment, the caliber of outflow tracts, and atrioventricular connections. The functional information comprised quantification of flow across valves, outflow tract, and defects. Cine imaging provided dynamic information of the cardiac size, valve morphology, leaflet mobility, wall thickness, chamber size, flow jets, outflow tracts, septum anatomy, defect morphology, and aortopulmonary connections. Stenosis or aneurysmatic dilatation of the great vessels was assessed on multiplanar reconstruction images and three-dimensional volume-rendered images of MRA.

During the radiologic assessment, extracardiac findings were also recorded. All the cardiovascular MRI examinations were evaluated according to the criteria listed in the guidelines and recommendations [5, 8–17].

### Statistical Analysis

The analysis of the obtained data was performed with SPSS version 20.0 software (IBM Corporation, Armonk, NY, USA). The mean and standard deviation values (mean $\pm$ SD) were used for the presentation of the descriptive values. Median values were also used for the body surface area and age of the patients.

## RESULTS

Cardiovascular MRI of 500 patients (M/F=301/199) was performed in radiology department between 2016 and 2019. The mean age of patients was 24.51 $\pm$ 18.14 years (median [IQR 25–75]; 17 [12–33]) and the mean body surface area was 1.58 $\pm$ 0.49 m<sup>2</sup> (median [IQR 25–75]; 1.6 [1.3–1.8]).

The most common indication for cardiovascular MRI was CHD (n=254, 50.8%). The other indications for cardiovascular MRI were myocardial disease (known or suspected ischemic, hypertrophic, restrictive, infiltra-

**TABLE 1.** Institutional protocol of cardiovascular MRI examination, and scan parameters

| Protocol                                  | Sequence                                      | Imaging plane  | Sequence parameters   |
|---|---|--|---|
| Localiser                                 | FIESTA (Non-cardiac gated)                    | Axial-coronal-sagittal plane   | TR 3 ms; TE 1 ms; flip-angle 60°; bandwidth ±111 kHz; matrix 224×224; FOV 350 mm; NEX 1; slice thickness 8 mm; gap 2 mm   |
| Protocol 1: Functional evaluation         | Cine b-SSFP                                   | 2-CH view*<br>4-CH view**<br>SA view***<br>LVOT and RVOT*                          | TR 3.6 ms; TE 1.5 ms; flip-angle 60°; bandwidth ±90 kHz; matrix 192×192; FOV 350 mm; NEX 1; slice thickness 8 mm; gap 0 mm  |
| Protocol 2: Blood flow assessment         | Phase-contrast imaging                        | AAO - level of RPA*<br>DAO- level of diaphragm*<br>MPA, RPA, and LPA*              | TR 5 ms; TE 3 ms; flip-angle 20°; bandwidth ±60 kHz; matrix 192×160; FOV 350mm; NEX 1; slice thickness 8 mm; gap 0 mm   |
| Protocol 3: Contrast-enhanced angiography | Tricks  | Coronal plane  | TR 4.2 ms; TE 1.4-11 ms; flip-angle 30°; bandwidth ±50 kHz; matrix 320×192; FOV 350 mm; NEX 1; slice thickness 8 mm; gap 0 mm   |
| Protocol 4: Late gadolinium enhancement   | PS-MDE  | Scout- SA view*<br>SA view***<br>Axial plane**                                     | A cine IR scout sequence to select the optimal inversion time for optimal suppression of healthy myocardium. 10 and 15 minutes post injection contrast agent TR 6.6 ms; TE 3.1 ms; flip-angle 25°; bandwidth ±62 kHz; matrix 192×192; FOV 350 mm; NEX 1; slice thickness 6 mm; gap 0 mm                             |
| Protocol 5: Tissue characterization       | T1 DIR<br>T2 DIR                              | SA view***<br>4-CH view**<br>SA view***<br>4-CH view**                             | Pre- and post-contrast, With and without fat saturation TR minimum; TE 35 ms; flip-angle 155°; bandwidth ±70 kHz; matrix 224×224; FOV 350 mm; NEX 1; slice thickness 6 mm; gap 0 mm<br>TR minimum; TE 102 ms; flip-angle 155°; bandwidth ±83 kHz; matrix 224×224; FOV 350 mm; NEX 1; slice thickness 6 mm; gap 0 mm |
| Protocol 6: Perfusion                     | Time course                                   | SA view***<br>Axial  | First pass bolus of contrast agent TR 3 ms; TE minimum; flip-angle 20°; bandwidth ±62.5 kHz; matrix 128x128; FOV 380 mm; NEX 1; slice thickness 8 mm; gap 10 mm   |
| Protocol 7: Iron load assessment          | Multi-TE GRE T2*                              | SA view***<br>4-CH view*   | TR 13.2 ms; TE 3, 7, 10, 14, 17, 20, 23, 26 and 29 ms; flip-angle 20°; bandwidth ±83.33 kHz; matrix 128×256; FOV 350 mm; NEX 1; slice thickness 6 mm; gap 15 mm   |
| Protocol 8: Vasculitis assessment         | T2 Black blood<br>T1 Black blood              | Coronal (thorax and abdomen)<br>Coronal (thorax and abdomen) pre and post-contrast | TR minimum; TE 60 ms; flip-angle 55°; bandwidth ±62.5 kHz; matrix 224×224; FOV 350 mm; NEX 1; slice thickness 8 mm; gap 2 mm<br>TR minimum; TE 20 ms; flip-angle 155°; bandwidth ±50 kHz; matrix 224×224; FOV 350 mm; NEX 1; slice thickness 8 mm; gap 2 mm   |
| Protocol 9: Coronary artery angiography   | 3D b-SSFP whole Heart (respiratory navigated) | Axial  | TR/TE minimum; flip-angle 65°; bandwidth ±100 kHz; matrix 224×224; FOV 350 mm; NEX 1; slice thickness 6 mm; overlap loc: 3, slap: 3   |

FIESTA: Fast imaging employing steady-state acquisition; 3D b-SSFP: Three dimensional balanced steady-state free precession; PS-MDE: Phase-sensitive myocardial delayed enhancement; IR: Inversion recovery; FOV: Field of view; CH: Chamber; SA: Short axis; RVOT: Right ventricular outflow tract; LVOT: Left ventricular outflow tract; AAO: Ascending aorta; DAO: Descending aorta; MPA: Main pulmonary artery; RPA: Right pulmonary artery; LPA: Left pulmonary artery.

tive, arrhythmogenic right ventricular, and noncompaction cardiomyopathy) (n=160, 32%), cardiac mass (n=44, 8.8%), valvular heart disease (n=20, 4%), MRA (n=12,

2.4% for aorta and pulmonary artery [n=9, 1.8%] and for coronary arteries [n=3, 0.6%]), vasculitis (n=7, 1.7%), and pericardial disease (n=3, 0.6%) (Fig. 1).

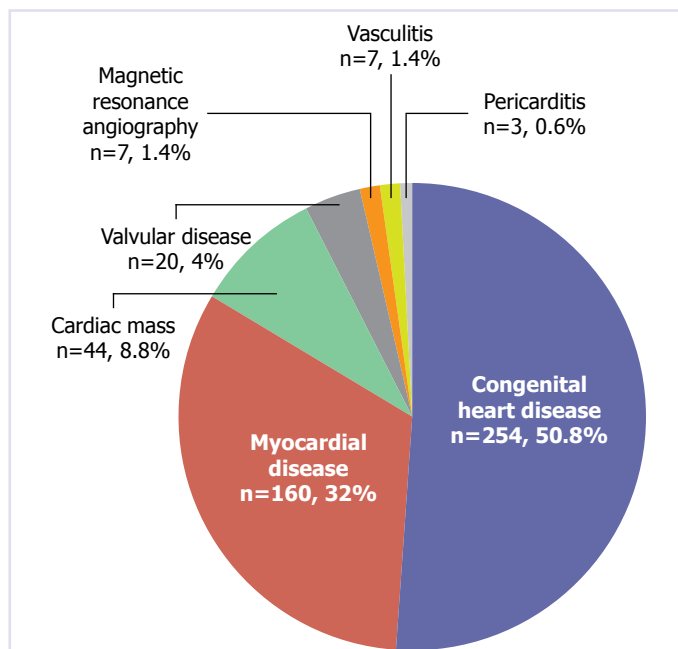


**FIGURE 1.** Frequency of indications for examination in all 500 cardiovascular MRIs. Myocardial assessment included ischemic and non-ischemic (hypertrophic, restrictive, infiltrative, arrhythmogenic right ventricular, and noncompaction cardiomyopathy) myocardial disease. Magnetic resonance angiography was included for great vessels and coronary arteries assessment.

The examination included functional imaging of the left and right ventricles was performed in all patients (100%). Detailed morphologic imaging of the heart was performed in 274 (54.8%), contrast-enhanced angiography of the great vessels was performed in 293 (58.6%), delayed-enhanced imaging for assessment for myocardial, pericardial disease, and vasculitis was performed in 208 (41.6%), and three-dimensional whole heart coronary angiography was performed in three patients (0.6%).

The most common indication for cardiovascular MRI was CHD ( $n=254$ ). The mean age of patients with CHD was  $16.47 \pm 9.91$  years (median [IQR 25–75]; 14 [11–18]). In CHD group, the most common diagnosis was repaired tetralogy of Fallot (TOF) in 202 patients (500/202; 40.4%). Among the patients with repaired TOF, 11 studies were performed for follow-up control study, and 23 patients were performed after pulmonary valve replacement. Cardiac MRI was performed for the assessment of post-surgical follow-up for transposition of great arteries in 11 patients (2.2%; seven patients had arterial switch surgery and four patients had double switch operation), Glenn procedure in seven patients

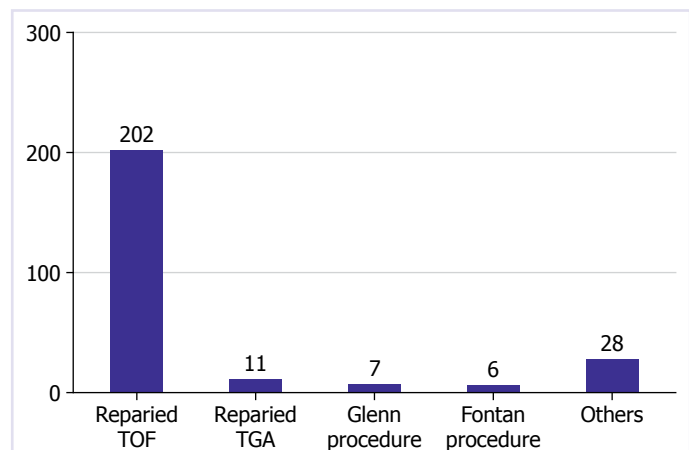


**FIGURE 2.** Frequency of the diagnosis of congenital heart disease in all 500 cardiovascular MRIs.

(1.4%), and Fontan procedure in six patients (1.2%) (Fig. 2). The other 28 patients (5.6%) with CHD had atrial septal defect ( $n=5$ ), ventricular septal defect ( $n=5$ ), partially anomalous pulmonary vein ( $n=4$ ), Ebstein's anomaly ( $n=3$ ), congenitally corrected transposition of great arteries ( $n=2$ ), patent ductus arteriosus ( $n=1$ ), apical band formation of left ventricle ( $n=1$ ), Keutel syndrome ( $n=1$ ), pulmonary lymphangiomatosis-congenital lobar emphysema ( $n=1$ ), cor triatriatum ( $n=1$ ), accessory tricuspid valve ( $n=1$ ), Uhl's anomaly ( $n=1$ ), isolated azygos continuation of inferior vena cava ( $n=1$ ), patent ductus arteriosus ( $n=1$ ), coarctation of aorta ( $n=1$ ), and truncus arteriosus ( $n=1$ ).

The second most frequent (32%) indication for cardiovascular MRI was myocardial disease. Among all myocardial disease ( $n=160$ ), T2\* sequence was performed to assess myocardial iron load without contrast agent injection in 35 patients (7%), and the mean T2\* value was found to be  $31.71 \pm 12.27$  ms (median [IQR 25–75]; 29 [22–40]). In the remaining 125 patients (25%), myocardial delayed enhancement imaging was performed. The most frequent indication for myocardial delayed enhancement imaging was left ventricular noncompaction cardiomyopathy ( $n=44$ , 8.8%) (Fig. 3); among these group, one patient had biventricular noncompaction cardiomyopathy (Fig. 4). The other indications were for hypertrophic cardiomyopathy in 38 patients (7.6%) (Fig. 5), arrhythmogenic right ventricular cardiomyopathy in 13 patients (2.6%) (Fig. 6), dilated cardiomyopathy in 6 patients (1.2%), myocarditis in eight patients (1.6%) (Fig. 7), myocardial storage disease in 11 patients (2.2%), ischemia related scar in two patients (0.4%), athlete heart,

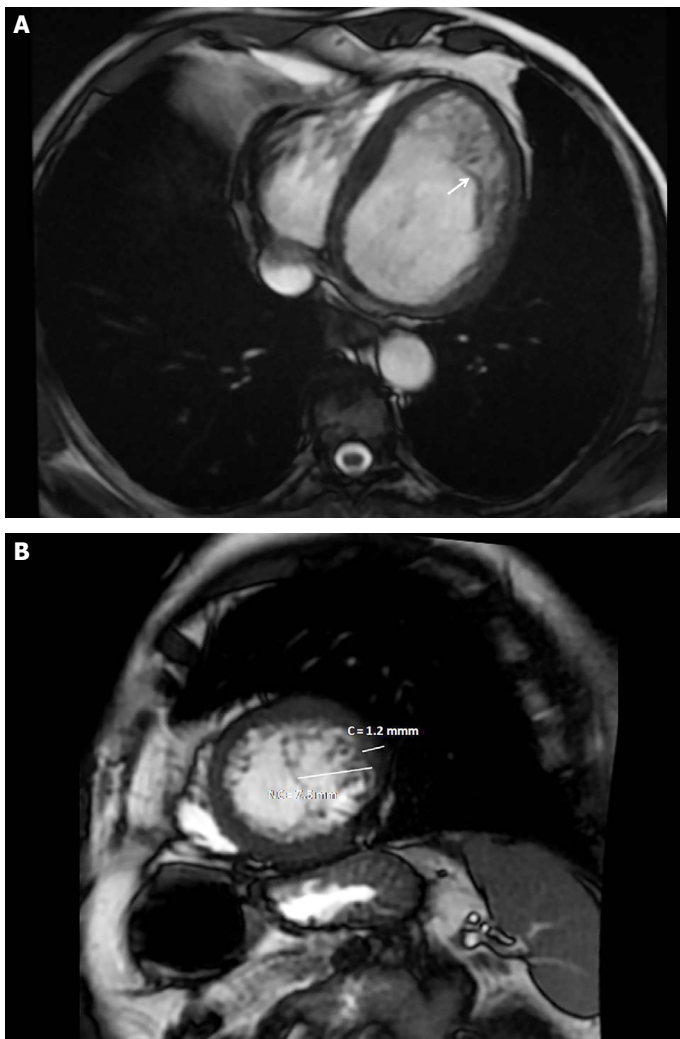


**FIGURE 3.** A 62-year-old male left ventricular noncompaction cardiomyopathy. Four chambers (**A**) and short-axis (**B**) bSSFP MRI in diastole shows increased subendocardial left ventricular trabeculation in the apical segment (arrow). The ratio of noncompacted (NC) to compacted [c] myocardial thickness is 6.2 (the mean ratio is 2.3). The ejection fraction was 41%.

myocardial contusion, and Takotsubo cardiomyopathy in one patient for each (0.2%). Among these patients, the indication was consistent with cardiac MRI findings in 84 patients (84/125, 67%). The characteristics of myocardial assessment and cardiovascular MRI diagnosis are showed in Figure 8.

The third most frequent indication for cardiovascular MRI was the assessment of cardiac mass in 44 patients (8.8%). Five patients with myxoma had surgical resection and were pathologically proved (Fig. 9). One patient had local cardiac invasion of known lung carcinoma, one pa-

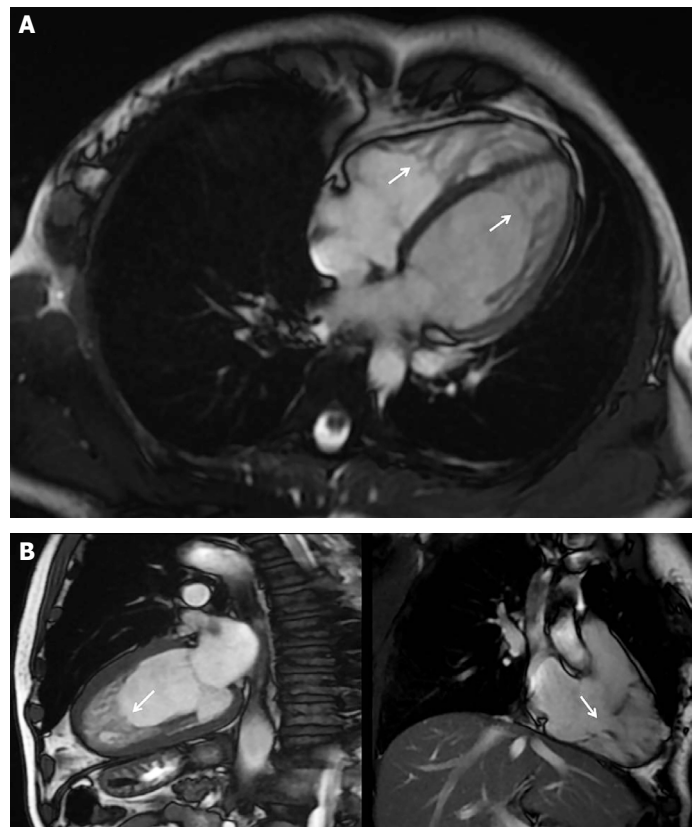


**FIGURE 4.** A 36-year-old female with biventricular noncompaction cardiomyopathy on four-chamber bSSFP MRI (arrows, **A**). Three-chamber bSSFP MRI of left (left) and right (right) ventricles show increased hypertrabeculation and noncompaction of right and left ventricles (arrows, **B**). The ejection fraction was 60% for the left ventricle and 58% for the right ventricle.

tient had a known surgical history of rhabdomyosarcoma, and one patient had a known history of ovarian leiomyomatosis. The remaining 36 patients, including eight patients with thrombus, were followed up and no major complications or morbidity were reported clinically and radiologically. Typical features of the cases with cardiac masses in their radiologic presentation, clinical and surgical features in our study cohort are reported in Table 2.

Three patients who underwent coronary artery assessment with three-dimensional whole heart MRA were evaluated for coronary artery anatomy instead of acquired coronary artery disease. Among nine patients who performed MRA for great vessels, five patients evaluated aortic diseases such as aneurysms or dissection. Aortic dimensions were assessed according to the criteria listed in multimodality imaging of diseases of the thoracic aorta in adults: From the American Society of Echocardi-

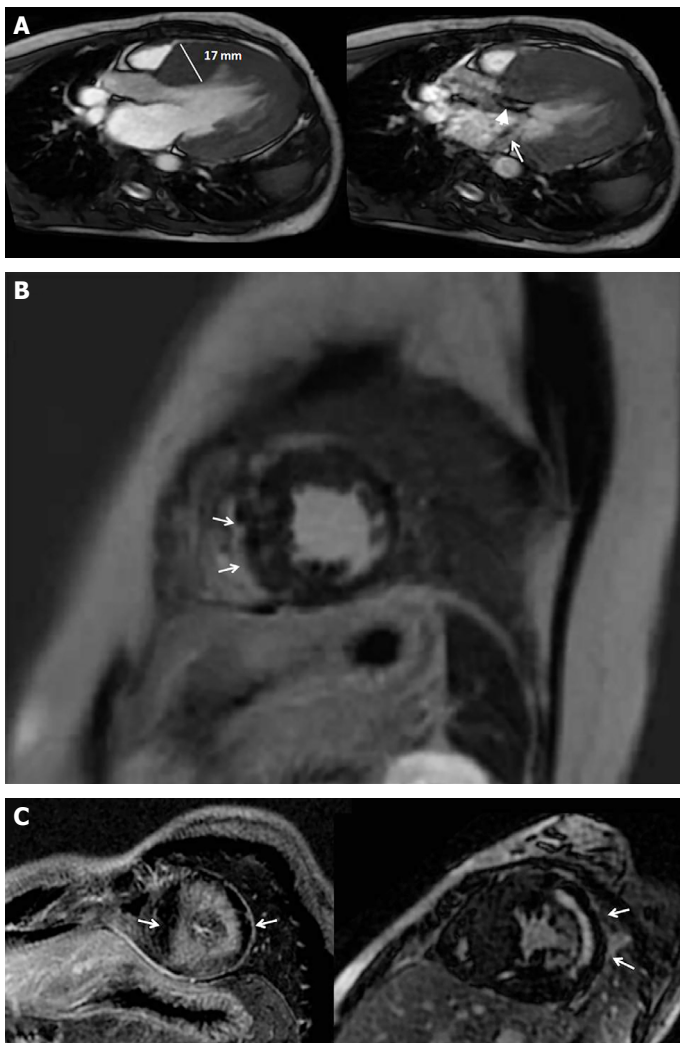


**FIGURE 5.** A 32-year-old male with a family history of sudden cardiac death. Three-chamber bSSFP MRI shows increased left ventricular wall thickness of more than 15 mm (line) on diastole (left), signal noise due to jet flow turbulence (arrow) in left ventricular outflow tract on systole, and systolic anterior motion of mitral valve (arrowhead) on systole (right) (**A**). Short-axis myocardial delayed enhancement MRI shows midwall patchy myocardial enhancement in interventricular septum (arrows, **B**). Short-axis myocardial delayed enhancement MRI shows extensive midwall enhancement in a 42-year-old male patient (left) and midwall myocardial enhancement in the lateral wall of the left ventricle (arrow) in a 24-year-old patient (right) (arrows, **C**).

ography and the European Association of Cardiovascular Imaging: Endorsed by the Society of Cardiovascular Computed Tomography and Society for Cardiovascular Magnetic Resonance [18]. The remaining four patients were assessed for pulmonary artery pathology and were found to have pulmonary artery sling in one patient, left

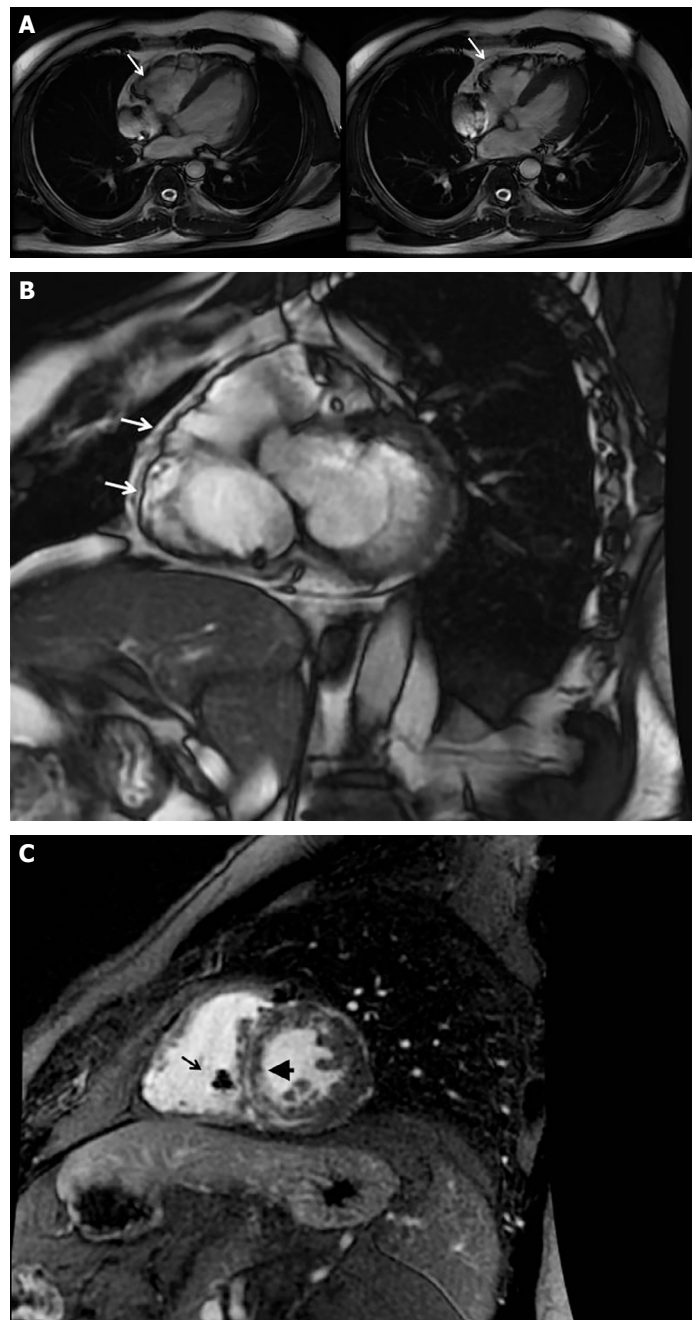


**FIGURE 6.** A 28-year-old male with arrhythmogenic right ventricular cardiomyopathy. Four-chamber bSSFP MRI shows dyskinesia an "accordion sign" in basal free wall caused by dyssynchronous contraction in the end-diastolic (arrow, left) and end-systolic (arrows, right) phase (**A**). Right ventricular outflow tract wall aneurysms in the short-axis bSSFP MRI (**B**, arrows). Late gadolinium enhancement MRI shows midwall myocardial enhancement in the septal wall (arrowhead) and mild enhancement of the right ventricular wall (**C**). The signal void in right ventricle is caused by metallic susceptibility artifact of intracardiac device (arrowhead, **C**).

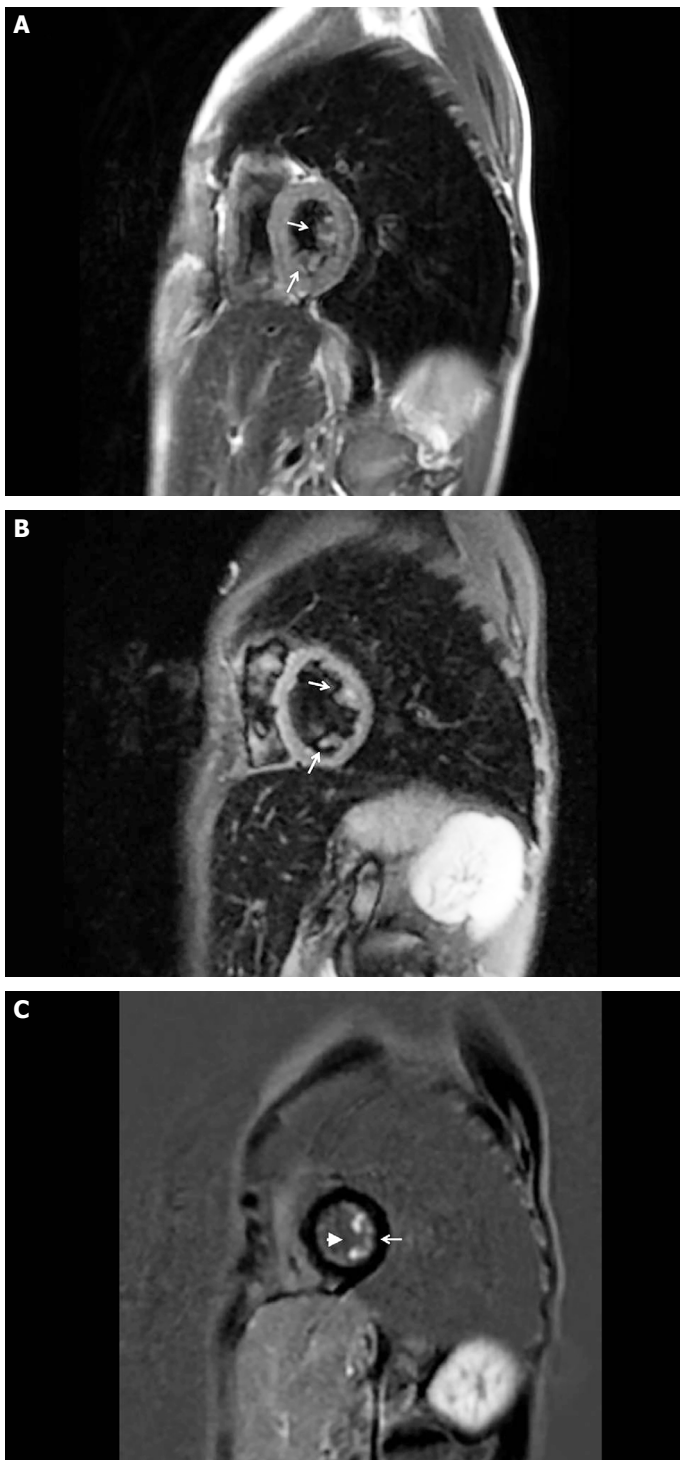


**FIGURE 7.** A 9-year-old boy with a medical history of bone marrow transplantation and cytomegalovirus endomyocarditis. Papillary muscles of the mitral valve show hypointensity on short-axis T1 weighted (arrow, **A**) and hyperintensity on short-axis T2 weighted (arrow, **B**) MRI. Myocardial delayed enhancement MRI shows patchy and multifocal sub-endocardial enhancement (arrow, **C**) and papillary muscle enhancement on the basal short-axis view (arrowhead, **C**).

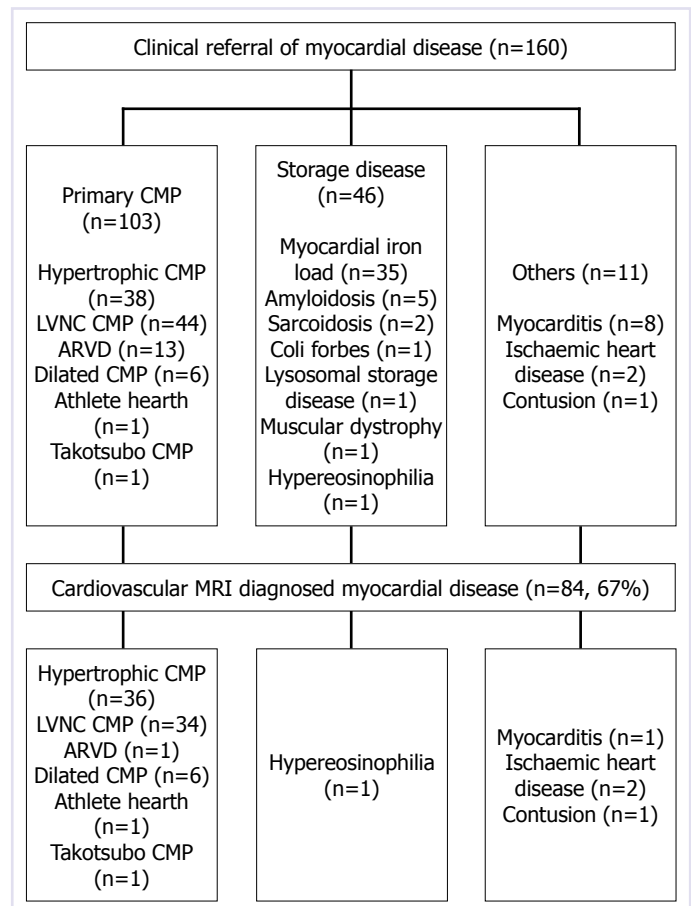


**FIGURE 8.** The characteristics of myocardial assessment and cardiovascular MRI diagnosis.

pulmonary artery agenesis in one patient, and pulmonary artery stenosis with Keutel syndrome in one patient. Twenty patients with valvular heart disease were assessed for aortic regurgitation. All the patients had bicuspid aortic valve (Fig. 10). In seven patients with the indication of vasculitis assessed for the segmental stenosis, mural irregularity, and contrast enhancement of vessel wall. Five patients had Takayasu arteritis, and the patients had been found to have segmenter stenosis in branches of the aortic arch, intimal irregularity, and contrast enhancement in the thoracic aorta. One patient had Behcet's disease, and one patient had middle aortic syndrome. In three patients with the indication of pericarditis, two patients were found to have constrictive pericarditis.

Major complication was not observed during the cardiovascular MRI examination. Three patients (0.06%) had minor complications during the contrast agent injection; one patient had pruritis, one patient had nausea, and one patient vomited. All patients were treated with pheniramine-maleate and dexamethasone.

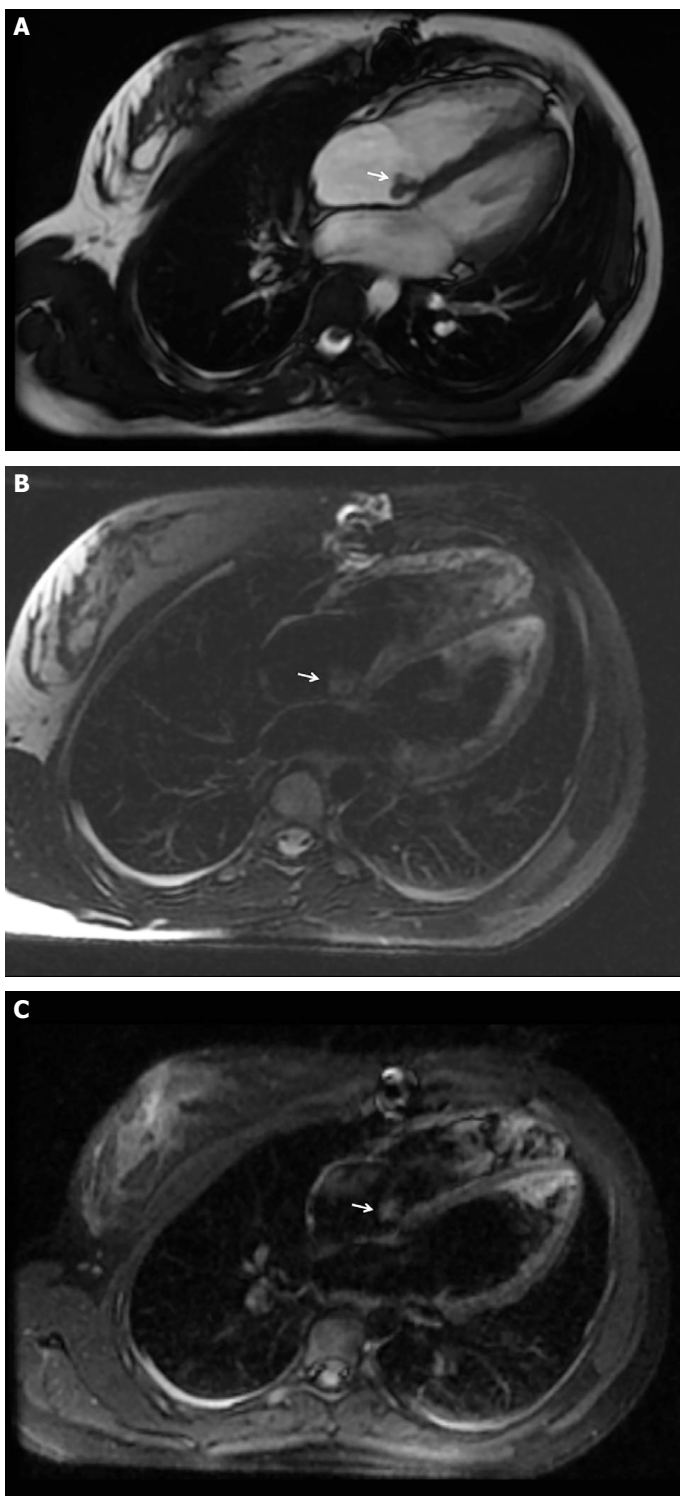
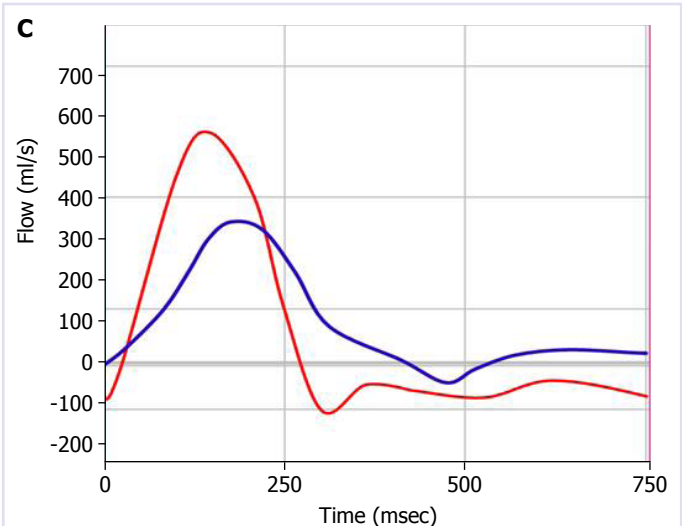
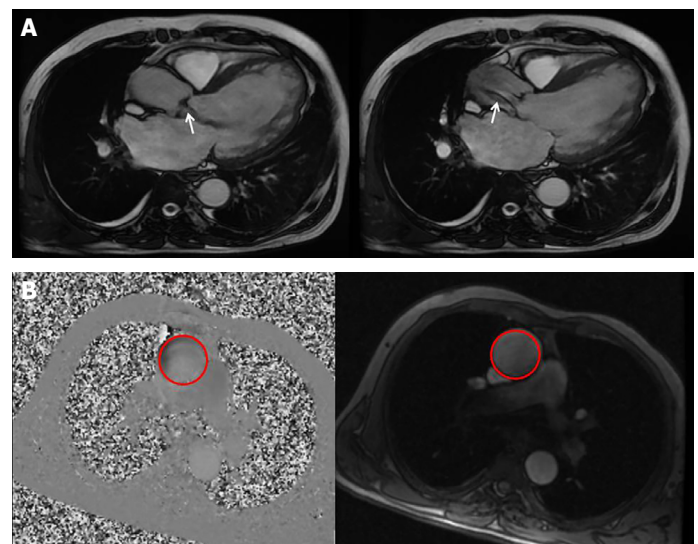


**FIGURE 9.** A 24-year-old female patient with myxoma. Solitary, well-defined, trilobulated mass in the right atrium arising from the interatrial septum near the fossa ovalis. The mass is hypointense on bSSFP **(A)** and mild hyperintense at T2-weighted MRI **(B)** (arrow). The mass had heterogeneous enhancement on myocardial delayed enhancement MRI **(C)** (arrow).



|                               |         |
|-------------------------------|---------|
| Peak positive velocity (cm/s) | 183.9   |
| Peak negative velocity (cm/s) | -111.9  |
| Flow (ml/min)                 | 4059    |
| Positive pixel flow (ml/min)  | 12640.5 |
| Negative pixel flow (ml/min)  | -8581.5 |

Summary: Flow 1-AAO

**FIGURE 10.** A 57-year-old male with the bicuspid aorta. Three-chamber bSSFP MRI of the left ventricular outflow tract shows backward flow turbulence in diastole consistent with aortic regurgitation (arrow, right) and forward flow turbulence in systole (arrow, left) consistent with aortic stenosis **(A)**. Phase (left) and magnitude images (right) of phase-contrast MRI revealed at ascending aorta **(B)**. Time-velocity curves of the ascending aorta (red curve) show regurgitant backward flow below the line. We calculated the aortic regurgitation fraction by dividing the regurgitant backward volume to forward flow **(C)**. The patient had a regurgitant fraction of 68% and an antegrade velocity of 1.8 m/s.

**TABLE 2.** Typical features of the cases with cardiac masses in their radiologic presentation, clinical and surgical features in our study cohort

| Cardiac mass (n=27)          | Location                                   | T2 weighted imaging | T1 weighted imaging | Contrast enhancement | Notes  |
|------------------------------|--|---------------------|---------------------|----------------------|--|
| Thrombus (n=8)               | Left auricle (n=7)<br>Left ventricle (n=1) | Hypo-isointense     | Hypo-isointense     | –                    | Resolved after anticoagulation therapy (confirmed by echocardiography)                 |
| Fibroma (n=2)                | Left ventricle mitral valve                | Hypo-isointense     | Hypo-isointense     | Peripheral           | Clinically followed-up   |
| Tuberculosis (n=3)           | Epi-pericardium                            | Hyper-isointense    | Hypo-isointense     | –                    | Amorph calcification on computed tomography, immunochemically proved                   |
| Epicardial cyst (n=1)        | Epi-pericardium                            | Hyperintense        | Hypointense         | –                    | Clinically followed-up   |
| Epicardial lipomatosis (n=2) | Epi-pericardium                            | Hyperintense        | Hyperintense        | –                    | Clinically followed-up   |
| Lipomatous hypertrophy (n=1) | Interatrial septum                         | Hyperintense        | Hyperintense        | –                    | Clinically followed-up   |
| Hemangioma (n=1)             | Left ventricle                             | Hyperintense        | Hyperintense        | +                    | Clinically followed-up   |
| Cyst hydatid (n=1)           | Epi-pericardium                            | Hyperintense        | Hypointense         | Peripheral           | Hypointense germinal membrane (T2-weighted imaging), confirmed by immunochemical tests |
| Myxoma (n=5)                 | Left article                               | Hyperintense        | Hypo-isointense     | +                    | Performed surgical resection   |
| Leiomyomatosis (n=1)         | Left ovarian vein to left pulmonary artery | Isointense          | Isointense          | +                    | Primary left ovarian leiomyomatosis  |
| Rhabdomyosarcoma (n=1)       | Left ventricle                             | Hyperintense        | Hypo-isointense     | +                    | Previous surgical resection  |
| Metastatic invasion (n=1)    | Adjacent to right atrium                   | Hyperintense        | Hypo-isointense     | +                    | Primary lung carcinoma performed surgical resection                                    |

Bigemini extrasystole was recorded in two patients (0.04%). One patient with arrhythmogenic right ventricular cardiomyopathy had intracardiac device on off-status during the examination and no complication was revealed.

Extra-cardiac findings occurred in roughly 9.2% (46/500) of the studies. 13 patients had double renal artery, nine patients had a gall bladder stone, seven patients had pleural effusion, two patients had atelectasis, one patient had surrenal gland mass, one patient had portal vein thrombosis, three patients had pericardial effusion, two patient had horseshoe kidney, one patient had a solitary kidney, one patient had pulmonary nodule, one patient had a splenic cyst, two patients isolated right kidney, one patient was found to have a thyroidal nodule, one patient had liver hemangioma, and one patient had lung cyst.

The duration of examination changed between 35 and 75 minutes depending on contrast agent injection.

## DISCUSSION

In the last few decades, cardiovascular MRI has been increasingly considered as a valuable modality for the assessment of large ranges of heart disease changes from myocardial diseases to CHD [19]. This retrospective, single-center experience study provides the clinical indications of cardiovascular MRI, imaging findings of cardiovascular disease, and institutional imaging protocols including CHD, myocardial disease, and cardiac masses.

In 2020, the indication of cardiovascular MRI with scanning techniques, clinical applicability, and adoption of cardiovascular MRI worldwide was updated and revised in the Society for Cardiovascular Magnetic Resonance consensus panel report by cardiologists and radiologists [5]. Our practice of cardiovascular MRI has been performed with the appropriateness of this consensus report. All of our patients were referred to our clinic by their cardiologist or cardiovascular surgeon before the cardiovascular MRI with the relevant indication.

Cardiovascular MRI has several advantages over other non-invasive diagnostic imaging techniques in the diagnosis, treatment, and monitoring of various heart diseases. The main advantage is that it does not contain ionizing radiation and does not require an iodinated contrast agent, which makes it a preferable imaging tool for patients with CHD in need of serial examinations during life-long follow-up. Imaging techniques with ionizing radiation have always posed a big challenge to clinicians in multiple, serial examinations either in the pre-operative and post-operative period. One of the most important roles of cardiovascular MRI is to establish a reference standard imaging tool with good reproducibility of right ventricular measurements for serial assessment, although retrosternal position and complex shape of the right ventricle which is difficult to assess in 2D-transthoracic echocardiography [5, 20]. The other advantage of cardiovascular MRI is blood flow analyses by phase-contrast imaging sequence. Phase-contrast imaging allows accurate, non-invasive, and radiation-free quantification of regurgitation fraction [21, 22] and pulmonary-to-systemic flow (Qp:Qs) ratio [23]. Proper selection of patients undergoing percutaneous pulmonary valve implantation such as TOF requires an accurate assessment of pulmonary regurgitation by contrast enhanced MRA [10]. Another important role of cardiovascular MRI in CHD is reliable visualization of vascular anatomy (aorta, pulmonary artery and pulmonary, pulmonary veins, etc.) has been recognized in the recent guideline [10]. Three-dimensional and multiplanar reconstruction imaging capabilities and large field of view make cardiac MRA an appropriate technique for the visualization for site, severity, the extension of the aneurysms or stenosis, and presence of collateral circulation [24]. Cardiovascular MRI angiography also provides important information in planning percutaneous or surgical intervention.

Although the technical difficulties (arrhythmia, the requirement of breath-holding, and need for anesthesia in infants) limit the application, all the major advantages make cardiovascular MRI an appropriate imaging tool in the assessment of CHD with the increasing use in specialized centers across the world. The European Society of Cardiology has suggested using cardiovascular MRI in patients with CHD for morphologic assessment of anomalies, evaluating thoracic aortic, conotruncal, and complex malformations, quantification of shunt lesions or regurgitation, and post-operative follow-up [25]. The main indication of cardiovascular MRI in our practice was CHD. Morphologic and anatomic structure of the

heart and great vessels, ventricular volume and function, the severity of shunt lesions, and valvular regurgitation were evaluated for all patients with CHD.

The assessment of myocardial disease was the second most frequent indication for cardiovascular MRI. Cardiovascular MRI is a well-established imaging tool in diagnosis and follow-up of myocardial diseases such as cardiomyopathies, myocarditis, and storage disease by providing accurate ventricular function and mass evaluation, non-invasive myocardial tissue characterization that can detect the presence and extend of myocardial edema and scarring. The pattern of contrast agent enhancement on late gadolinium enhancement sequences may point toward the etiology, prognosis, and severity of the cardiomyopathy [13, 26]. Cardiovascular MRI also can be used either in the acute phase and chronic myocarditis. In the acute phase of myocarditis, inflammatory changes can be evaluated by a T2-weighted imaging sequence [27]. And also, in chronic myocarditis, the transformation of the inflammatory response to myocardial fibrosis by late gadolinium enhancement sequence [28]. CMR also plays a crucial role in imaging and managing the patients at high risk (those with  $T2^* < 10$  ms) undergone repeated transfusions and assessing response the chelation therapy [17].

Cardiovascular MRI offers an accurate diagnostic value of left ventricular non-compaction cardiomyopathy in the visualization of ventricular anatomy and trabecula with an increased high spatial, temporal, and contrast resolution [5, 29]. In arrhythmogenic right ventricular cardiomyopathy, CMR-based criteria including regional wall motion abnormalities with increased right ventricular volume and impaired ejection fraction must be present for the diagnosis [30].

The second most frequent indication for cardiovascular MRI was myocardial disease during our experience. Myocardial delayed enhancement imaging was performed in almost 78% of the myocardial assessment. T2\* sequence was performed to assess myocardial iron load without contrast agent injection in the remaining 22% of patients. In 85% of the patients, the indication was consistent with cardiac MRI findings. We believe that cardiovascular MRI has the capability to answer the clinical questions including volume, function, viability, inflammatory response, and cardiomyopathy with excellent image quality.

Cardiovascular MRI also is being increasingly considered an imaging tool for the assessment of morphol-

ogy, tissue composition, localization, invasive growth, and metastatic spreading, and hemodynamic relevance of cardiac tumors that define the therapeutic management [31, 32]. Serial cardiovascular MRI studies can be used to follow-up for suspected tumoral lesions or monitor response to chemotherapy or radiotherapy [33, 34]. Cardiac mass was the third most frequent indication during our clinic. Among these patients, eight patients had surgical resection and pathological-ly proved. The remaining 36 patients (36/44, 81.8%), including eight patients with thrombus, were followed up clinically and radiologically no major complications or morbidity were reported. Merged imaging and clinical findings can be used in tumor stratification and clinical decision in practice.

The other indications for cardiovascular MRI were valvular heart disease (n=20, 4%), MRA (n=12, 2.4% for aorta and pulmonary artery [n=9, 1.8%] and for coronary arteries [n=3, 0.6%]), vasculitis (n=7, 1.7%), and pericardial disease (n=3, 0.6%). In our study, the amount of the indication for vascular (aorta, pulmonary artery, and coronary artery) pathologies, pericarditis, and vasculitis was limited.

Coronary MRA has been rapidly developing over the past few years. The most crucial advantage of coronary MRA is that it technically does not require contrast material and does not contain ionizing radiation. However, long acquisition time and metallic susceptibility artifact by a stent, prosthetic valve, etc., are the main limitations of the technique [35]. The role of the coronary MRA is explained as assessment of the anomalous origin and proximal course and the presence of fistula or aneurysm by expert consensus [32]. All the patients were evaluated for coronary artery anatomy rather than atherosclerotic coronary artery disease.

Transthoracic echocardiography still remains the first choice technique in valvular heart diseases. Cardiovascular MRI is recommended when echocardiography provides insufficient information. On cardiovascular MRI, valvular anatomy and function, stenosis in inflow and outflow tracts can be assessed by cine bSSFP sequence. However, the major advantage of cardiovascular MRI over echocardiography is quantifying flow and regurgitation fraction [5]. In our study cohort, the patients examined for valvular disease had bicuspid aorta and assessed for aortic regurgitation. Besides that, all the patients with CHD assessed for valvular function, regurgitation, or stenosis.

The ability to null blood signal with post-contrast T1 weighted imaging provides important opportunities for identifying vasculitis and inflammatory changes in the aorta and its branches [32, 36]. In our study group, seven patients with the indication of vasculitis were found to have segmental stenosis, mural irregularity, and contrast enhancement of vessel wall. Since it was stated that MRA with fat-saturated T1-weighted imaging could be used to evaluate activity and response to treatment [37], we suggested post-treatment follow-up evaluation.

The average time-duration of the examination was between 35 and 75 min depending on contrast agent injection. A contrast agent was needed for MRA and myocardial delayed enhancement images; additional scanning time was approximately 15 min for both. In this large group of patients, a few minor complications occurred and were resolved without the need for hospitalization.

Cardiac MRI has various study-independent limitations such as long scanning times, patient noncooperation, claustrophobia, limited availability, and high cost. Advanced scanning techniques would be preferred to minimize the artifacts secondary to arrhythmias and metallic objects. Cardiac devices are one of the main limitations of MRI examination. Although cardiac MRI is known contraindicated in the patients with a pacemaker or implantable cardio defibrillator because of the risk of device dysfunction and possible heating or voltage effects during scanning, it's reported that no long-term clinically significant adverse events were reported during the scanning of 1509 patients with pacemaker or a legacy implantable cardioverter or defibrillator system in a recent article [38]. One patient with cardiac device was scanned. However, we have not recorded that how many appointments were cancelled because of claustrophobia and the intracardiac devices. Stress perfusion cardiovascular MRI with stress agents (dobutamine, adenosine, dipyridamole, etc.) has a widely accepted application in the evaluation of suspected coronary artery disease and enables the evaluation of the perfusion difference between normal and hypoperfused myocardium and coronary artery reserve through delayed contrast wash-in evaluation [32, 39]. However, we did not perform stress perfusion cardiovascular MRI because of the technical difficulties. The main reason for this limitation is the complications (bronchoconstriction, arrhythmia,

myocardial ischemia or infarction, and nausea/vomiting) of stress agent requires the presence of a cardiovascular imaging team includes a cardiologist and nurse. On the other hand, stress agents did not approved for use in radiology clinic in Türkiye. Majority of cardiac MRI is currently being performed on 1.5 Tesla MRI systems. 3.0 Tesla, and in some centers 7.0 Tesla MRI systems are now being used for clinical and research application by increased signal-to-noise ratio and resolution with decreased examination time. In higher strength, MRI systems various technologies are performed to adapt the ECG changes and breath hold requirements. However, susceptibility artifacts remain the major limitation for cardiac MRI at higher strength MRI systems [40].

The most important limitation of this study is its retrospective, single-center design. The other limitation is that the management of the study and examinations performed by the observer trained in congenital cardiac imaging. This may have led to the referral of patients with predominantly CHD. Multicenter studies with larger patient cohorts combined adult and pediatric ages will enhance the experience, clinical use, and impact of cardiovascular MRI.

## Conclusion

Cardiovascular MRI is a reliable and accurate imaging tool in identifying the various cardiac pathology with widely accepted use in clinical areas. Our single-center experience of 500 cases demonstrates the varieties of clinical indications in daily practice may contribute to the national data pool. We believe that increased collaboration between radiologists and clinicians will enhance the clinical use of cardiovascular MRI, future development of imaging protocol and reporting systems.

**Ethics Committee Approval:** The Istanbul Medeniyet University Clinical Research Ethics Committee granted approval for this study (date: 12.12.2018, number: 2018/0483).

**Conflict of Interest:** No conflict of interest was declared by the authors.

**Financial Disclosure:** The authors declared that this study has received no financial support.

**Authorship Contributions:** Concept – SO, IKY; Design – SO; Supervision – SO, IKY; Fundings – SO, IKY; Materials – SO, IKY; Data collection and/or processing – SO, IKY; Analysis and/or interpretation – SO, IKY; Literature review – AC, AS; Writing – SO; Critical review – SO, AC, AS.

## REFERENCES

1. Pattynama PM, De Roos A, Van der Wall EE, Van Voorthuisen AE. Evaluation of cardiac function with magnetic resonance imaging. *Am Heart J* 1994;128:595–607. [CrossRef]
2. Sakuma H, Fujita N, Foo TK, Caputo GR, Nelson SJ, Hartiala J, et al. Evaluation of left ventricular volume and mass with breath-hold cine MR imaging. *Radiology* 1993;188:377–80. [CrossRef]
3. Klein C, Nekolla SG, Bengel FM, Momose M, Sammer A, Haas F, et al. Assessment of myocardial viability with contrast-enhanced magnetic resonance imaging: comparison with positron emission tomography. *Circulation* 2002;105:162–7. [CrossRef]
4. Gutberlet M, Fröhlich M, Mehl S, Amthauer H, Hausmann H, Meyer R, et al. Myocardial viability assessment in patients with highly impaired left ventricular function: comparison of delayed enhancement, dobutamine stress MRI, end-diastolic wall thickness, and TI201-SPECT with functional recovery after revascularization. *Eur Radiol* 2005;15:872–80. [CrossRef]
5. Leiner T, Bogaert J, Friedrich MG, Mohiaddin R, Muthurangu V, Myerson S, et al. SCMR Position Paper (2020) on clinical indications for cardiovascular magnetic resonance. *J Cardiovasc Magn Reson* 2020;22:76. [CrossRef]
6. Boxt LM, Rozenshtein A. MR imaging of congenital heart disease. *Magn Reson Imaging Clin N Am* 2003;11:27–48. [CrossRef]
7. Pignatelli RH, McMahon CJ, Chung T, Vick GW 3<sup>rd</sup>. Role of echocardiography versus MRI for the diagnosis of congenital heart disease. *Curr Opin Cardiol* 2003;18:357–65. [CrossRef]
8. Weber OM, Higgins CB. MR evaluation of cardiovascular physiology in congenital heart disease: flow and function. *J Cardiovasc Magn Reson* 2006;8:607–17. [CrossRef]
9. Baumgartner H, De Backer J, Babu-Narayan SV, Budts W, Chessa M, Diller GP, et al; ESC Scientific Document Group. 2020 ESC Guidelines for the management of adult congenital heart disease. *Eur Heart J* 2021;42:563–645. [CrossRef]
10. Stout KK, Daniels CJ, Aboulhosn JA, Bozkurt B, Broberg CS, Colman JM, et al. 2018 AHA/ACC guideline for the management of adults with congenital heart disease: a report of the American College of Cardiology/American Heart Association Task Force on Clinical Practice Guidelines. *J Am Coll Cardiol* 2019;73:e81–192. Erratum in: *J Am Coll Cardiol* 2019;73:2361–2.
11. Di Salvo G, Miller O, Babu Narayan S, Li W, Budts W, Valsangiacomo Buechel ER, et al; 2016–2018 EACVI Scientific Documents Committee. Imaging the adult with congenital heart disease: a multimodality imaging approach-position paper from the EACVI. *Eur Heart J Cardiovasc Imaging* 2018;19:1077–98. [CrossRef]
12. Parwani P, Co M, Ramesh T, Akhter N, Iliescu C, Palaskas N, et al. Differentiation of cardiac masses by cardiac magnetic resonance imaging. *Curr Cardiovasc Imaging Rep* 2020;13. [CrossRef]
13. Lee E, Ibrahim EH, Parwani P, Bhave N, Stojanovska J. Practical guide to evaluating myocardial disease by cardiac MRI. *AJR Am J Roentgenol* 2020;214:546–56. [CrossRef]
14. te Riele AS, Tandri H, Bluemke DA. Arrhythmogenic right ventricular cardiomyopathy (ARVC): cardiovascular magnetic resonance update. *J Cardiovasc Magn Reson* 2014;16:50. [CrossRef]
15. Friedrich MG, Sechtem U, Schulz-Menger J, Holmvang G, Alakija P, Cooper LT, et al; International Consensus Group on Cardiovascular Magnetic Resonance in Myocarditis. Cardiovascular magnetic resonance in myocarditis: a JACC White Paper. *J Am Coll Cardiol* 2009;53:1475–87. [CrossRef]

16. Petersen SE, Selvanayagam JB, Wiesmann F, Robson MD, Francis JM, Anderson RH, et al. Left ventricular non-compaction: insights from cardiovascular magnetic resonance imaging. *J Am Coll Cardiol* 2005;46:101–5. [[CrossRef](#)]
17. Messroghli DR, Moon JC, Ferreira VM, Grosse-Wortmann L, He T, Kellman P, et al. Clinical recommendations for cardiovascular magnetic resonance mapping of T1, T2, T2\* and extracellular volume: a consensus statement by the Society for Cardiovascular Magnetic Resonance (SCMR) endorsed by the European Association for Cardiovascular Imaging (EACVI). *J Cardiovasc Magn Reson* 2017;19:75. Erratum in: *J Cardiovasc Magn Reson* 2018;20:9. [[CrossRef](#)]
18. Goldstein SA, Evangelista A, Abbara S, Arai A, Asch FM, Badano LP, et al. Multimodality imaging of diseases of the thoracic aorta in adults: from the American Society of Echocardiography and the European Association of Cardiovascular Imaging: endorsed by the Society of Cardiovascular Computed Tomography and Society for Cardiovascular Magnetic Resonance. *J Am Soc Echocardiogr* 2015;28:119–82.
19. Valsangiacomo Buechel ER, Grosse-Wortmann L, Fratz S, Eichhorn J, Sarikouch S, Greil GF, et al. Indications for cardiovascular magnetic resonance in children with congenital and acquired heart disease: an expert consensus paper of the Imaging Working Group of the AEPIC and the Cardiovascular Magnetic Resonance Section of the EACVI. *Eur Heart J Cardiovasc Imaging* 2015;16:281–97. [[CrossRef](#)]
20. Grothues F, Moon JC, Bellenger NG, Smith GS, Klein HU, Pennell DJ. Interstudy reproducibility of right ventricular volumes, function, and mass with cardiovascular magnetic resonance. *Am Heart J* 2004;147:218–23. [[CrossRef](#)]
21. Rebergen SA, Chin JG, Ottenkamp J, van der Wall EE, de Roos A. Pulmonary regurgitation in the late postoperative follow-up of tetralogy of Fallot. Volumetric quantitation by nuclear magnetic resonance velocity mapping. *Circulation* 1993;88:2257–66. [[CrossRef](#)]
22. Wald RM, Redington AN, Pereira A, Provost YL, Paul NS, Oechslin EN, et al. Refining the assessment of pulmonary regurgitation in adults after tetralogy of Fallot repair: should we be measuring regurgitant fraction or regurgitant volume? *Eur Heart J* 2009;30:356–61. [[CrossRef](#)]
23. Beerbaum P, Körperich H, Barth P, Esdorn H, Gieseke J, Meyer H. Noninvasive quantification of left-to-right shunt in pediatric patients: phase-contrast cine magnetic resonance imaging compared with invasive oximetry. *Circulation* 2001;103:2476–82. [[CrossRef](#)]
24. Konen E, Merchant N, Provost Y, McLaughlin PR, Crossin J, Paul NS. Coarctation of the aorta before and after correction: the role of cardiovascular MRI. *AJR Am J Roentgenol* 2004;182:1333–9. [[CrossRef](#)]
25. von Knobelsdorff-Brenkenhoff F, Schulz-Menger J. Role of cardiovascular magnetic resonance in the guidelines of the European Society of Cardiology. *J Cardiovasc Magn Reson* 2016;18:6. [[CrossRef](#)]
26. Cummings KW, Bhalla S, Javidan-Nejad C, Bierhals AJ, Gutierrez FR, Woodard PK. A pattern-based approach to assessment of delayed enhancement in nonischemic cardiomyopathy at MR imaging. *Radiographics* 2009;29:89–103. [[CrossRef](#)]
27. Vashist S, Singh GK. Acute myocarditis in children: current concepts and management. *Curr Treat Options Cardiovasc Med* 2009;11:383–91. [[CrossRef](#)]
28. Gagliardi MG, Bevilacqua M, Di Renzi P, Picardo S, Passariello R, Marcelletti C. Usefulness of magnetic resonance imaging for diagnosis of acute myocarditis in infants and children, and comparison with endomyocardial biopsy. *Am J Cardiol* 1991;68:1089–91. [[CrossRef](#)]
29. Alhabshan F, Smallhorn JF, Golding F, Musewe N, Freedom RM, Yoo SJ. Extent of myocardial non-compaction: comparison between MRI and echocardiographic evaluation. *Pediatr Radiol* 2005;35:1147–51. [[CrossRef](#)]
30. Marcus FI, McKenna WJ, Sherrill D, Basso C, Bauce B, Bluemke DA, et al. Diagnosis of arrhythmogenic right ventricular cardiomyopathy/dysplasia: proposed modification of the Task Force Criteria. *Eur Heart J* 2010;31:806–14. [[CrossRef](#)]
31. Butany J, Nair V, Naseemuddin A, Nair GM, Catton C, Yau T. Cardiac tumours: diagnosis and management. *Lancet Oncol* 2005;6:219–28.
32. Hundley WG, Bluemke DA, Finn JP, Flamm SD, Fogel MA, Friedrich MG, et al; American College of Cardiology Foundation Task Force on Expert Consensus Documents. ACCF/ACR/AHA/NASCI/SCMR 2010 expert consensus document on cardiovascular magnetic resonance: a report of the American College of Cardiology Foundation Task Force on Expert Consensus Documents. *J Am Coll Cardiol* 2010;55:2614–62. [[CrossRef](#)]
33. Poterucha TJ, Kochav J, O'Connor DS, Rosner GF. Cardiac tumors: clinical presentation, diagnosis, and management. *Curr Treat Options Oncol* 2019;20:66. [[CrossRef](#)]
34. Fussen S, De Boeck BW, Zellweger MJ, Bremerich J, Goetschalckx K, Zuber M, et al. Cardiovascular magnetic resonance imaging for diagnosis and clinical management of suspected cardiac masses and tumours. *Eur Heart J* 2011;32:1551–60. [[CrossRef](#)]
35. Sakuma H. Coronary CT versus MR angiography: the role of MR angiography. *Radiology* 2011;258:340–9. [[CrossRef](#)]
36. Treitl KM, Maurus S, Sommer NN, Kooijman-Kurfuerst H, Coppenrath E, Treitl M, et al. 3D-black-blood 3T-MRI for the diagnosis of thoracic large vessel vasculitis: a feasibility study. *Eur Radiol* 2017;27:2119–28. [[CrossRef](#)]
37. Jiang L, Li D, Yan F, Dai X, Li Y, Ma L. Evaluation of Takayasu arteritis activity by delayed contrast-enhanced magnetic resonance imaging. *Int J Cardiol* 2012;155:262–7. [[CrossRef](#)]
38. Pennell DJ. Cardiovascular magnetic resonance and the role of adenosine pharmacologic stress. *Am J Cardiol* 2004;94:26D–31. [[CrossRef](#)]
39. Nazarian S, Hansford R, Rahsepar AA, Weltin V, McVeigh D, Gucuk Ipek E, et al. Safety of magnetic resonance imaging in patients with cardiac devices. *N Engl J Med* 2017;377:2555–64. [[CrossRef](#)]
40. Auti OB, Bandekar K, Kamat N, Raj V. Cardiac magnetic resonance techniques: our experience on wide bore 3 tesla magnetic resonance system. *Indian J Radiol Imaging* 2017;27:404–12. [[CrossRef](#)]